論文 / 著書情報
Article / Book Information

題目(和文)	
Title(English)	Radial-velocity search and statistical studies for short-period planets in the Pleiades open cluster
著者(和文)	宝田拓也
Author(English)	Takuya Takarada
出典(和文)	学位:博士(理学), 学位授与機関:東京工業大学, 報告番号:甲第11057号, 授与年月日:2019年3月26日, 学位の種別:課程博士, 審査員:佐藤 文衛,中本 泰史,井田 茂,野村 英子,玄田 英典
Citation(English)	Degree:Doctor (Science), Conferring organization: Tokyo Institute of Technology, Report number:甲第11057号, Conferred date:2019/3/26, Degree Type:Course doctor, Examiner:,,,,
学位種別(和文)	博士論文
Category(English)	Doctoral Thesis
種別(和文)	要約
Type(English)	Outline

Dissertation outline

Radial-velocity search and statistical studies for short-period planets in the Pleiades open cluster

Department of Earth and Planetary Sciences
Tokyo Institute of Technology
Takuya Takarada

1 INTRODUCTION

1.1 Diversity of exoplanets

Over 3,000 planets have been discovered since the discovery of the first known exoplanet, 51 Pegasi b (Mayor & Queloz, 1995). The increasing number of detections helps to understand the statistical properties of planets and develop theoretical models of planetary formation and evolution.

Figure 1 shows the distribution of exoplanets on a mass–period plane. We can see that giant planets with masses greater than 0.3 $M_{\rm JUP}$ and orbital periods between 1–10 d are clustered, which we call hot Jupiters (HJ). However, the formation and evolution of HJs still is not completely understood.

One of the reasons why understanding the origins of HJs has been difficult is the age of the systems at which the HJs were discovered. Most of the planets detected by the RV and transit methods are orbiting old main-sequence stars in the age groups of >1 Gyr. In the meantime, the number of planets discovered around younger stars is small.

1.2 Mechanism of hot Jupiter formation

In the standard core-accretion scenario, giant planets are formed beyond the snow line, far from the central star, where there exists plenty of solid materials to form the massive solid cores of giant planets. The existence of HJs suggest there should be some mechanism by which the giant planets are displaced from their birthplace to the vicinity of their central star. Two leading models are proposed to explain the formation of HJs – gas disk migration (GDM, so-called Type-II migration) and high-eccentricity tidal migration (HEM). In GDM, the young giant planet creates a gap in the protoplanetary disk and moves inward through the gap (e.g. Goldreich & Tremaine 1980). HJs formed with this mechanism are considered to have nearly close-in circular orbits. In HEM, giant planets are scattered through gravitational interaction with other companions on high-eccentricity orbits that evolve into close-in circular orbits through a tidal interaction with the central star (e.g., Rasio & Ford 1996).

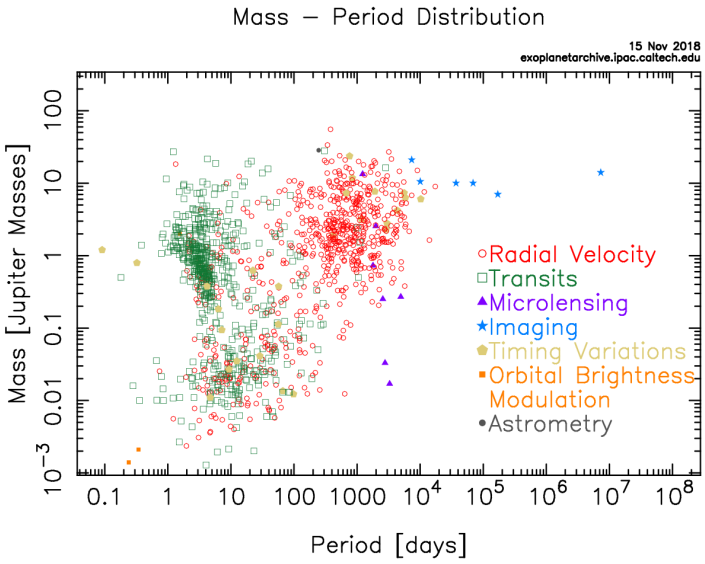

Figure 1: Exoplanet mass as a function of orbital period. Each color denotes the detection method and the corresponding meaning is shown in the right-bottom corner. This figure is retrieved from NASA Exoplanet Archive (https://exoplanetarchive.ipac.caltech.edu).

The crucial factor to discriminate between GDM and HEM is the time-scale over which HJs are formed by the respective mechanisms. In GDM, the planet migration has to be completed before the dissipation of the protoplanetary disk, and the timescale of HJ formation is determined by the lifetime of the disk ($\lesssim$ 10 Myr, Haisch et al. 2001). In HEM, planet scattering and tidal circularization take hundreds of Myr to form the final shape of the system. Therefore, the planet survey targeting stars in the age groups of approximately 100 Myr will help to distinguish between GDM and HEM. However, such approaches have not yet been successful due to the large stellar surface activities on young stars (e.g., Lagrange et al. 2013).

1.3 Paucity of massive HJs around solar-type stars

The paucity of massive HJs (MHJ) orbiting solar-type stars has been reported in transit surveys. MHJs with masses greater than 5 $M_{\rm JUP}$ were preferentially detected around hotter stars.

Several studies tried to reproduce the distribution with numerical simulations. Bouchy et al. (2011) for instance suggested that close-in massive planets around G-type dwarfs might be engulfed due to the loss of angular momentum caused by magnetic braking and tidal interactions. On the other hand, those orbiting early and mid F-type dwarfs can escape the engulfment since they are rapid rotators with small outer convective zones, and thus they do not produce tidal forces strong enough to cause an angular momentum loss in the planets.

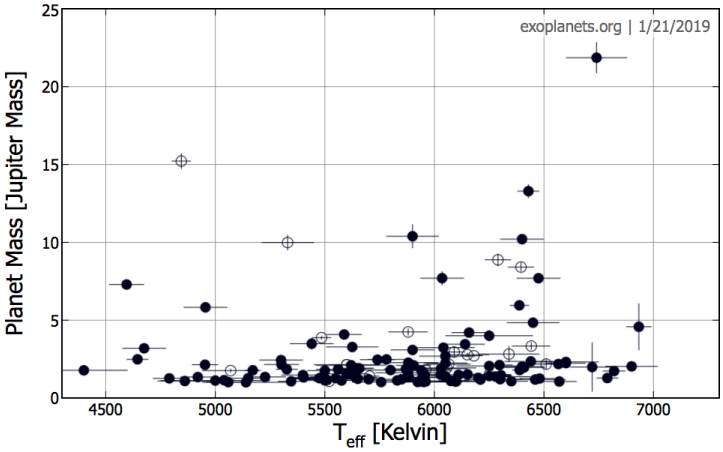

Figure 2: The mass of planet as a function of the host star's effective temperature. Filled and open circles correspond to planets with orbital periods from 1–5 and 5–10 days, respectively. The color range on the right denotes the masses of host star. We only plotted planets of masses greater than 1 $M_{\rm JUP}$.

1.4 Planet survey in open cluster

Both observational and theoretical works have tried to understand the formation and evolution of HJs. The common factors preventing the comprehension of these processes are the age of the stars and the uncertainties pertaining it. To overcome this problem, surveys in open clusters should be one of the most effective approaches.

So far 26 planets have been discovered in open clusters. Although several HJs have been discovered in open clusters, these clusters are relatively old ($\gtrsim$600 Myr), and the constraint on the formation and evolution mechanism of HJs has been inconclusive. In the K2 mission, some young open clusters (Pleiades, M 18, M 21, M 25, and M 35) in age groups less than 200 Myr were observed. Up until today, no planets have been discovered in these observations.

1.5 Motivation of this thesis

As described in the previous section, information on the age groups of open clusters where the exoplanets were found are not young enough to investigate the formation and evolution of HJs. To set a stringent constraint on the HJ formation mechanism, the ages of open clusters are preferred to be less than ~ 0.1 Gyr. Planet surveys in younger open clusters can also help to investigate HJ evolution, and particularly the paucity of MHJ.

On these grounds, we performed a HJ survey in the Pleiades open cluster (~ 0.1 Gyr) using RV methods. By determining the occurrence rate of HJs in the Pleiades, this study aims to set constraints on their formation and evolution.

The reasons why we chose the Pleiades cluster are its young age and close proximity to our solar

system. Due to the age of the cluster, we can set more stringent constraints on the timescale of formation of HJs. Pleiades is the second nearest open cluster to our solar system. Therefore, it is possible to observe relatively bright stars, which allows us to perform precise RV measurements.

2 OBSERVATIONS

2.1 Sample selection

We selected sample stars in the Pleiades open cluster based on the following criteria: i) the membership probability is over 70% (Kharchenko et al. 2004; Bouy et al. 2015); ii) visual (V) magnitude is approximately 9.4–10.5; and, iii) the spectral type is between F8 and G5. We selected fifty stars based on the criteria and among those observed thirty.

The aim of our observations is to prove the presence or absence of HJs around young stars. To achieve this, we planned to observe each star approximately 5 times – three observations at consecutive nights and more than two observations over an interval of several days. Although we could not obtain five pieces of data for some stars, we made at least three consecutive observations for them, which is still useful to explore very short period planets ($<$3 d).

2.2 Observation

All data were obtained with the 1.88-m reflector and High Dispersion Echelle Spectrograph (HIDES; Izumiura et al. 1999; Kambe et al. 2013) at the Okayama Astrophysical Observatory (OAO). An iodine absorption cell (I_2 cell; Kambe et al. 2002) was set on the optical path, which superposes numerous iodine absorption lines onto a stellar spectrum of 5000–5800 Å as the fiducial wavelength reference for precise RV measurements.

2.3 Data reduction

Reduction of echelle data was done on IRAF. We go along the flow chart in Figure 3.

3 ANALYSIS

3.1 Radial velocity

3.1.1 Computation of radial velocity

We compute RV variations following the method described in Sato et al. (2002) based on the ones established by Valenti et al. (1995) and Butler et al. (1996). In this method, the observed spectrum (I_2-

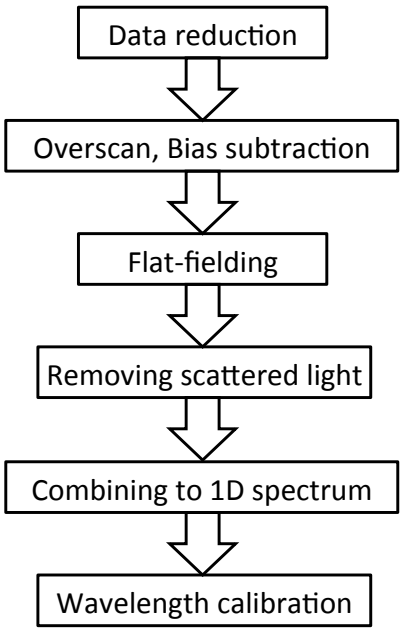

Figure 3: Flow chart of IRAF reduction

superposed stellar spectrum) is modeled using a stellar template spectrum and high-resolution I_2 spectrum, both of which are convolved with the instrumental profile (IP) of the spectrograph.

We used the spectra obtained by other instruments as stellar template spectra. Among our sample, ten and five stars were observed through High Accuracy Radial Velocity Planet Searcher (HARPS) with the 3.6 meter telescope at La Silla and High Resolution Echelle Spectrometer (HIRES) with the 10 meter telescope at Keck Observatory, respectively. Additionally, we obtained the spectra of eight stars through High Dispersion Spectrograph (HDS) with the 8.2 meter telescope at Subaru Telescope. Excluding the duplication, we could collect template spectra for 15 stars.

3.1.2 Rotational velocity

To determine a template spectrum for stars without pure spectra, we derived the rotational velocity of our sample. We fitted the observed spectra covering 6400–6500 Å with theoretical spectra made by SPECTRUM code (Gray & Corbally, 1994). The chemical composition of the model spectra is assumed to be identical to that of the Sun. The fitting parameters are the rotational velocity, $v \sin i$, Doppler shift, and a linear normalization function. Figure 4 shows how the stellar rotation affect on the profile of stellar absorption lines.

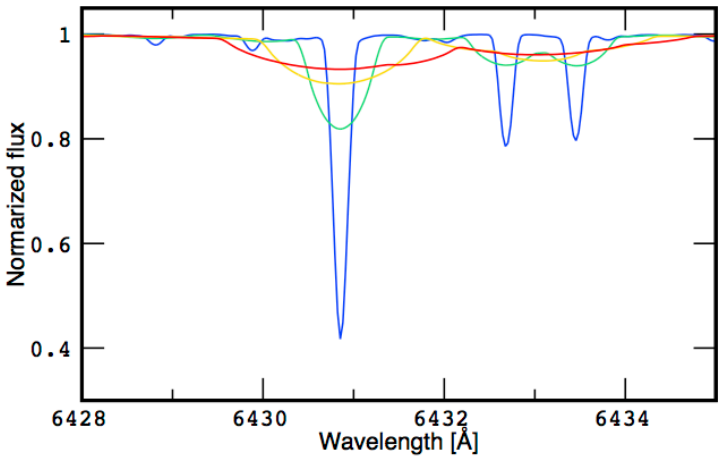

Figure 4: Spectra broadened by stellar rotation. Blue, green, yellow, and red lines correspond to the rotational velocities, $v \sin i$, of 5, 20, 40, and 60 km s^{-1}, respectively.

3.2 Line profile analysis

3.2.1 Least-squares deconvolution

Each absorption line has low SNR, which prevents the precisely evaluation of the line-profile deformations. Therefore, we adopted a technique to enhance the SNR of the line-profile. For this purpose, we computed a mean stellar absorption line profile with the use of the least-squares deconvolution (LSD) method following Kochukhov et al. (2010).

3.2.2 Indices of line profile deformation

To monitor the line-profile deformation, we computed three line-profile indices from a mean line profile; the FWHM, $V_{\rm span}$, and $W_{\rm span}$.

The FWHM is computed by fitting a line profile with a Gaussian profile. Boisse et al. (2011) proposed $V_{\rm span}$ as the indicator of line asymmetry. $V_{\rm span}$ is defined as the velocity difference of two Gaussian profiles. One Gaussian profile is fitted to a line-wing region, and other Gaussian profile is fitted to a line-core region. $W_{\rm span}$ is proposed by Santerne et al. (2015), which is an alternate asymmetry diagnosis to $V_{\rm span}$. $W_{\rm span}$ is also defined as a velocity difference of two Gaussian profiles. One Gaussian profile is fitted to a line blue-wing region, and the other Gaussian profile is fitted to a line red-wing region.

3.3 Hα line

We check the flux variability of Hα line core at 6562.808 Å. Hα line is used to check chromospheric activities. Boisse et al. (2011) showed the correlation between RV and several activity indicators, including Hα line core flux, for an active K2V star. We define Hα index, $S_{\mathrm{H}\alpha}$, as

$$S_{\mathrm{H}\alpha} = \frac{F_{\mathrm{H}\alpha}}{F_{\mathrm{B}} + F_{\mathrm{R}}}, \tag{1}$$

where $F_{\mathrm{H}\alpha}$ is the integrated flux within a 1.6-Å-wide bin centered at Hα line, and F_{B}, F_{R} is a 6.0-Å-wide bin centered at 6552.3 Å and 6574.8 Å, respectively.

3.4 Statistical analysis

3.4.1 Detection limit and search completeness

The detection limit – the upper limit of detectable planetary masses at a given orbital period – gives important information that will help to establish the presence of HJs. Following Meunier et al. (2012), we compute the detection limit with the root-mean-square (RMS) method.

Next, we compute the search completeness, C, by stacking the detection limits of our sample (Howard et al., 2010). The search completeness shows the fraction of stars from which we can detect planets with a given mass and orbital period if present.

3.4.2 Planet occurrence rate

We compute the planet occurrence rate following Borgniet et al. (2017). For the first step, we compute the integrated search completeness, C_I, over a specific parameter range, $[m_{p1} : m_{p2}]$ and $[P_1 : P_2]$, defined as

$$C_I = \frac{\sum_{P_1}^{P_2} \sum_{m_{p1}}^{m_{p2}} \left(\frac{1}{N} \sum_{i=1}^{N} \delta_i \right) \mathrm{d}P \, \mathrm{d}m_p}{\sum_{P_1}^{P_2} \sum_{m_{p1}}^{m_{p2}} 1 \, \mathrm{d}P \, \mathrm{d}m_p}. \tag{2}$$

To account for the search incompleteness, we estimate the number of missed planets, n_{miss}, defined as

$$n_{\mathrm{miss}} = n_{\mathrm{det}} \times \left(\frac{1}{C_I} - 1 \right) \tag{3}$$

where n_{det} is the number of detected planets within the specific parameter range. Although we did not detect any planets in our survey, we defined $n_{\mathrm{det}} = 1$ following Borgniet et al. (2017).

Then we compute the planet occurrence rate with the use of binomial statistics.

4 RESULTS

4.1 Radial-velocity variations and activity indicators

4.1.1 Rotational velocity

We derived rotational velocities for our sample. We found that larger V magnitude stars tend to have slower rotational velocities. This is consistent with previous studies (Queloz et al., 1998).

4.1.2 Radial-velocity measurement errors

We found that σ_{RVerr} exceeds 100 $\mathrm{m\,s^{-1}}$ for stars with $v \sin i \geq 30$ $\mathrm{km\,s^{-1}}$. When compared with the expected σ_{RVerr}, the observed σ_{RVerr} seems to be worse by a factor of 2–5. This indicates that there might be some factors that led to the gap between the RV measurement errors and the expected errors.

There can be two possible factors causing the discrepancy of RV errors. Firstly, the stellar template mismatch could be a matter of RV precision for stars for which we used template spectra of different stars. Secondly, the wavelength-dependent stellar activities may also worsen the RV precision. If each stellar absorption line profile were subjected to different deformations, the velocity variance of each segment would increase.

4.1.3 Radial-velocity variabilities

We found that four stars exhibit large RV variations when compared to the RV measurement errors. The large RV variations could be caused by planets or stellar activities. In the next section, we examine the causes of the large RV variations.

4.1.4 Activity indicators

To evaluate the effect of stellar activities on RV variations, we computed FWHM, $\mathrm{S_{H\alpha}}$, $\mathrm{V_{span}}$ and $\mathrm{W_{span}}$ for our sample. For each star, the strong correlation between RV and FWHM, V_{span} and W_{span} are seen. For these reasons, we conclude that the significant RV variations seen from the four stars were caused by stellar activities and no planet candidates were detected among our sample.

4.2 Statistical analysis

We computed the detection limits for our sample. When we found a significant correlation between the RVs and activity indicators, we fitted a linear function to the correlation and subtracted it to mitigate the effect of stellar activity on RV variations. After that, we computed the detection limit again. By performing the correction of stellar activity, the mass limit came down to approximately 1 M_{JUP} in the same range. In this way, we could improve the detection limit by a factor of 2–3.

By combining the detection limits of our sample, we derived the search completeness of our survey. Since stars with high rotational velocities show large RV measurement errors, we divided our sample into two sub-samples; 18 stars with $v \sin i < 20$ km s^{-1} and 12 stars with $v \sin i > 20$ km s^{-1} to examine the search completeness for less massive planets. We can see a remarkable improvement for the sub-sample of rapidly rotating stars. Although the completeness is worse than the sub-sample of slowly rotating stars, the correction lets us rule out massive close-in planets ($\sim 10\ M_{\rm JUP}$). From the whole sample, we can see that our observation rules out the existence of massive HJs with orbital periods of $1-5$ day.

We derived the planet occurrence rate from our survey. We divide the mass and period ranges into two groups, respectively: 1–5 $M_{\rm JUP}$ and 5–13 $M_{\rm JUP}$ for mass, and 1–5 day and 5–10 day for orbital period. In the domain of the less massive planets (1–5 $M_{\rm JUP}$), the completeness is less compared to the domain of the massive planets. In the meantime, our survey distinctly investigates the domain of massive planets. This indicates that RV-measurement precisions are sufficient to confidently rule out the existence of such planets among our sample.

5 DISCUSSION

5.1 Stellar radial-velocity jitter

Based on the analysis of RV and activity indicators, we evaluate the stellar RV jitter of the Pleiades stars. The values we derived are consistent with those obtained by other surveys targeting open clusters as young as the Pleiades; 128 m s^{-1} for NGC 2422 (73 Myr, Bailey et al. 2018), 67 m s^{-1} for NGC 2516 (141 Myr, Bailey et al. 2018), 58 m s^{-1} for Castor moving group (200$\pm$100 Myr, Paulson & Yelda 2006) and 65 m s^{-1} for Ursa Major moving group (300 Myr, Paulson & Yelda 2006).

5.2 Planet occurrence rate

Although the planet occurrence rate derived from our sample gave us a constraint on the HJs population around young stars, we attempted to enforce a more stringent constraint by combining our results with those obtained by other surveys targeting young clusters. For this purpose, we referred to Paulson & Yelda (2006) (P06) and Bailey et al. (2018) (B18). P06 observed four young open clusters and moving groups by the RV method; β Pic association ($\sim$12 Myr), IC 2391 (30–50 Myr), Castor moving group (200$\pm$100 Myr) and Ursa Major moving group (300 Myr). We do not refer to β Pic association due to its poor constraints on the detection limit. B18 derived the detection limits for 117 stars in NGC 2516 (141 Myr) and NGC 2422 (73 Myr) based RV observations.

6 SUMMARY

We conducted a radial-velocity search for short-period planets in the Pleiades open cluster to investigate their formation and evolution process. The observations were done between November and December 2017 at Okayama Astrophysical observatory with High Dispersion Echelle Spectrograph.

Firstly, we computed the RVs for our sample and found that the RV measurement error was worse than expected. Although we have not yet fully clarified the cause of degradation, the wavelength-dependent stellar activities might provide a partial explanation. We also computed several stellar activity indicators as well as RV measurements. Several stars showed significant RV variations compared to RV measurement errors. By comparing RVs with the activity indicators, we found strong correlations between them and concluded that these RV variations were caused by stellar activities. From our observations, no planet candidates were detected. For stars exhibiting RV variations by stellar activities, we fitted a linear function to the correlation and subtracted it from the RV values to mitigate stellar intrinsic RV variations.

Secondly, we performed a statistical analysis on our sample. By correcting the effect of stellar activities on RVs, the detection limits were improved by a factor of 2–3. Then, we combined the detection limits of whole samples and derived the search completeness for our survey. We divided our sample into two sub-samples based on stellar rotational velocities. We then derived the planet occurrence rate in the Pleiades open cluster. Our observations set a constraint on the occurrence rate of planets in the Pleiades for the first time.

By combining our survey with two other surveys targeting the open clusters in the age groups of 30–300 Myr, we attempted to enforce a more stringent constraint on the planet occurrence rate with an orbital period of 3 days. To take the difference of the detection sensitivities of each survey into account, we divided the planet masses into three ranges; 1–5, 5–13, and 13–80 $M_{\rm JUP}$. The lack of detection of massive short-period planets might indicate that such planets are originally less likely to be formed around solar-type stars.

References

Bailey, J. I., Mateo, M., White, R. J., Shectman, S. A., & Crane, J. D. 2018, MNRAS, 475, 1609

Boisse, I., Bouchy, F., Hébrard, G., et al. 2011, A&A, 528, A4

Borgniet, S., Lagrange, A.-M., Meunier, N., & Galland, F. 2017, A&A, 599, A57

Bouchy, F., Deleuil, M., Guillot, T., et al. 2011, A&A, 525, A68

Bouy, H., Bertin, E., Sarro, L. M., et al. 2015, A&A, 577, A148

Butler, R. P., Marcy, G. W., Williams, E., et al. 1996, PASP, 108, 500

Goldreich, P., & Tremaine, S. 1980, ApJ, 241, 425

Gray, R. O., & Corbally, C. J. 1994, AJ, 107, 742

Haisch, K. E., Jr., Lada, E. A., & Lada, C. J. 2001, ApJ, 553, L153

Izumiura, H. 1999, Observational Astrophysics in Asia and its Future, 77

Kambe, E., Sato, B., Takeda, Y., et al. 2002, PASJ, 54, 865

Kambe, E., Yoshida, M., Izumiura, H., et al. 2013, PASJ, 65, 15

Kochukhov, O., Makaganiuk, V., & Piskunov, N. 2010, A&A, 524, A5

Kharchenko, N. V., Piskunov, A. E., Röser, S., Schilbach, E., & Scholz, R.-D. 2004, Astronomische Nachrichten, 325, 740

Lagrange, A.-M., Meunier, N., Chauvin, G., et al. 2013, A&A, 559, A83

Mayor, M., & Queloz, D. 1995, Nature, 378, 355

Meunier, N., Lagrange, A.-M., & De Bondt, K. 2012, A&A, 545, A87

Paulson, D. B., & Yelda, S. 2006, PASP, 118, 706

Queloz, D., Allain, S., Mermilliod, J.-C., Bouvier, J., & Mayor, M. 1998, A&A, 335, 183

Rasio, F. A., & Ford, E. B. 1996, Science, 274, 954

Santerne, A., Díaz, R. F., Almenara, J.-M., et al. 2015, MNRAS, 451, 2337

Sato, B., Kambe, E., Takeda, Y., Izumiura, H., & Ando, H. 2002, PASJ, 54, 873

Valenti, J. A., Butler, R. P., & Marcy, G. W. 1995, PASP, 107, 966